Macromolecules

ARTICLE

pubs.acs.org/Macromolecules

Linear Rheological Response of a Series of Densely Branched Brush Polymers

Miao Hu,[†] Yan Xia,[‡] Gregory B. McKenna,*[,†] Julia A. Kornfield,*[,‡] and Robert H. Grubbs[‡]

[†]Department of Chemical Engineering, Texas Tech University, Lubbock, Texas 79409, United States

[‡]Division of Chemistry and Chemical Engineering, California Institute of Technology, Pasadena, California 91125, United States

ABSTRACT: We have examined the linear rheological responses of a series of well-defined, dense, regularly branched brush polymers. These narrow molecular weight distribution brush polymers had polynorobornene backbones with degrees of polymerization (DP) of 200, 400, and 800 and polylactide side chains with molecular weight of 1.4 kDa, 4.4 kDa, and 8.7 kDa. The master curves for these brush polymers were obtained by time temperature superposition (TTS) of the dynamic moduli over the range from the glassy region to the terminal flow region. Similar to other long chain branched polymers, these densely branched brush polymers show a sequence of relaxation. Subsequent to the glassy relaxation, two different relaxation processes can be observed for samples with the high molecular weight (4.4 and 8.7 kDa) side chains, corresponding to the relaxation of the side chains and the brush polymer backbone. Influenced by the large volume fraction of high molecular weight side chains, these brush polymers are unentangled. The lowest plateau observed in the dynamic response is not the rubbery entanglement plateau but is instead associated with the steady state recoverable compliance. Side chain properties affect the rheological responses of these densely branched brush polymers and determine their glassy behaviors.

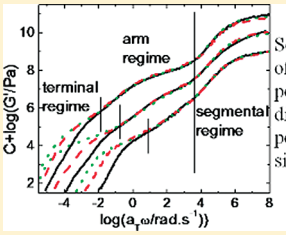

Sequential relaxation of dense brush polymers having different degree of polymerization and side chain lengths

INTRODUCTION

Polymer architecture has long been known to greatly affect the rheological properties of polymer materials. Brush polymer is a unique type of graft polymers possessing a very high density of regularly spaced side chains along the backbone, and has become a subject of active research in the field of molecular rheology due to its interesting architecture.[1−20] The grafting density and the molecular weight of the branches affect the movement of the backbone and the rheological responses of these complex macromolecules.

The rheological responses of long chain branched polymers with relatively low grafting density have been well examined.[1−12] In general, such polymers relax in a sequence with the grafted branches relaxing first, followed by the branching points, and the backbone subsequently reptates in a dilated tube.[1,3] Side chains act as a solvent and decrease the rubbery modulus of the backbone.[3,12] For polymers with shorter side chains and extremely high grafting density, similar to the long chain branched polymers, two rubbery plateaus are found in the dynamic master curves.[14−20] One corresponds to the relaxation of the side chains. A second, lower plateau with modulus value of approximately 1 kPa is usually regarded as the rubbery plateau of the whole polymer.[13,14,16,19] It is found that the modulus value of the lower plateau decreases with increasing side chain length and the entanglement molecular weights (M_e) of these densely branched brush polymers are extremely high.[16] The very low rubbery modulus is attributed to the interactions between the densely packed side chains which causes the polymer backbones to be stiffened as the persistence length of the brush chain increases with increasing side chain density.[13,15,16,21−23] A worm-like conformation is expected for this kind of brush polymer.[13,24,25] The stiffened chain conformation affects the inter chain interactions and increases the distance between entanglements. Prior studies were limited by the synthesis methods available to polymers with high backbone degree of polymerization (DP) but side chain length generally lower than 1/4 of the entanglement molecular weight of the corresponding linear polymer.[14,16,19] There are no prior systematic works investigating how the side chain length and backbone DP affect the rheological responses of the densely branched brush polymers. In the present investigation we take advantage of a new type of densely grafted brush polymer with narrow molecular weight distribution that is synthesized via ring-opening metathesis polymerization (ROMP) of macromonomers (MMs).[26,27] The resulting brush polymers possess low polydispersities (PDIs) in both backbones and side chains, and very high molecular weights (up to 6000 kDa). The MM synthetic approach ensures that each repeat unit in the backbone is grafted with a side chain, leading to very large branch to backbone ratios and a dense distribution of branching points.[23,24,26−28] We have synthesized polynorbornene-*g*-polylactide brush polymers with polylactide side chain length of 1/5, 1/2, and 1 entanglement distance of the corresponding linear polymer and the backbone degree of polymerization (DP) of 200, 400, and 800. In the following section, we first present our experimental methods and then show the results of dilute solution characterization of these densely branched brush polymers. This is followed by a presentation of the dynamic moduli

Received: April 27, 2011
Revised: July 24, 2011
Published: August 04, 2011

ACS Publications © 2011 American Chemical Society

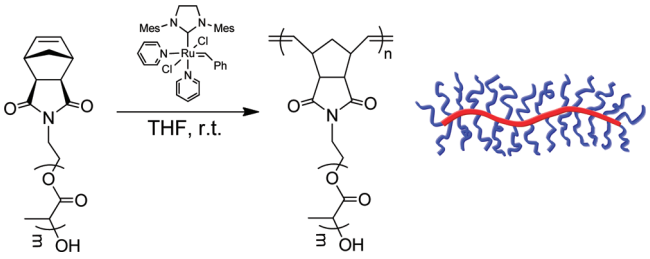

Figure 1. Scheme of the synthesis of polynorbornene-*g*- polylactide brush polymers and schematic of the resulting brush polymer.

Table 1. Sample Molecular Weight and Characterization Data

sample number	M_{br} [a] (kDa)	DP [b]	M_w [c] (kDa)	PDI [d]	φ_{br} [e]
P(PLA1.4)-200	1.4	200	350	1.01	0.893
P(PLA1.4)-400		400	680	1.02	0.898
P(PLA1.4)-800		800	1510	1.04	0.900
P(PLA4.4)-200	4.4	200	840	1.02	0.951
P(PLA4.4)-400		400	2240	1.02	0.956
P(PLA4.4)-800		800	4880	1.03	0.958
P(PLA8.7)-200	8.7	200	1600	1.02	0.970
P(PLA8.7)-400		400	3660	1.08	0.975
P(PLA8.7)-800		800	6050	1.07	0.977

[a] M_{br} is the molecular weight of the side chains. [b] DP is the degree of polymerization of the backbone. [c] M_w is the molecular weight of the brush polymer determined by GPC−MALLS in THF. [d] Polydispersity index (PDI) of the brush polymer. [e] φ_{br} is the volume fraction of the side chain estimated by the group contribution method.[31]

of the materials and the temperature dependence of the dynamics. We then discuss the sequential relaxation of these densely branched brush polymers covering the three ranges from the glassy relaxation through the Rouse-like relaxation regime of the side chains through the terminal regime which also shows the hallmark of unentangled Rouse-like behavior in spite of the high backbone DP of 800. Similar to what was originally shown by Plazek,[29,30] the steady state recoverable compliance contributes to the long time dynamics of these unentangled or barely entangled materials.

EXPERIMENT

Polymer Synthesis. The polynorbornene-*g*-poly-(D,L)-lactide brush polymers used in this study were synthesized by previously described ring-opening metathesis polymerization (ROMP) of norbornenyl macromonomers (MMs) (Figure 1).[26] The molecular weights of the MMs and the brush polymers were controlled by the ratio of the monomer (or MM) to the initiator (see Table 1).

Gel Permeation Chromatography (GPC). GPC was carried out in THF on two PLgel 10 μm mixed-B LS columns (Polymer Laboratories) connected in series with a DAWN EOS multiangle laser light scattering (MALLS) detector, an Optilab DSP differential refractometer, and a ViscoStar viscometer (all from Wyatt Technology). No calibration standards were used, and dn/dc values of 0.050 for PLA brush polymers were obtained by assuming 100% mass elution from the columns.

Rheological Measurements. These were carried out using an MCR-501 rheometer (Anton Paar Inc.) with 8 mm parallel plate and approximately 1 mm gap under nitrogen flow over a temperature range from 50 to 140 °C. The measured frequency range is 0.01−100 Hz. The machine compliance was corrected by setting both the cell compliance and geometry compliance in the instrument software to zero and the raw data were corrected using the measured machine compliance value following Hutcheson and McKenna's method.[32] The dynamic responses at different temperature were shifted and the master curve of $G'(\alpha_T\omega)$ and $G''(\alpha_T\omega)$ vs $\alpha_T\omega$ was constructed at a reference temperature of 80 °C. When constructing the master curves, the same shift factors were applied to each group of samples with the same side chain molecular weights. To determine the shift factors for each group of samples, the shift factors for the 400DP polymers were chosen as the reference and modified a little to find the best fit values for the other two samples. For samples with longer side chains, some empirical vertical shifting was applied to shift the dynamic curves at different temperatures together. Creep experiments were performed at 80 °C in the 8 mm parallel plate geometry. The experiments were carried out until steady state was achieved and the viscosity was determined. The steady state recoverable compliance was determined by subtracting time divided by viscosity from the creep compliance.[33]

DATA ANALYSIS

Fragility and Glass Transition Temperature. The shift factors with reference temperature at 80 °C were fitted with the WLF equation.[34]

$$\log(a_T) = \frac{-c_1(T - T_{ref})}{c_2 + T - T_{ref}} \quad (1)$$

The C_1 and C_2 at this reference temperature (T_{ref}) were estimated from the curve fitting. According to the principle of time (frequency)-temperature superposition, the temperature dependence of the $G'(\omega)$ and $G''(\omega)$ ($G'(\omega)$ and $G''(\omega)$ vs T) at the frequency of ω = 0.0628 rad/s was converted from the dynamic master curve ($G'(\omega)$ and $G''(\omega)$ vs ω) with the WLF equation and used to determine the glass transition temperature (T_g). T_g was estimated from the peak of the tan(δ) curve in the so-constructed dynamic modulus thermal spectrum. We fit the shift factors with the WLF equation at the reference temperature set to T_g to estimate the C_1^g and C_2^g. The fragility (m)[35−37] and apparent activation energy (E_g) of the brush samples were estimated with equations,[38,39]

$$m = \frac{c_1^g T_g}{c_2^g} \quad (2)$$

$$E_g = \ln 10\, R \frac{c_1^g}{c_2^g} T_g^{\,2} \quad (3)$$

The change of C_1^g, C_2^g, T_∞, fragility (m), apparent activation energy (E_g), and glass transition temperature (T_g) of the brush polymers are discussed subsequently.

Retardation Spectrum. According to Plazek,[29,30] the retardation spectrum ($L(\tau)$) is a very useful tool to examine the relaxation behavior of polymer chains. The retardation spectrum can be calculated from the dynamic results or creep data. To calculate the retardation spectrum ($L(\tau)$) from the dynamic data, the relaxation spectrum ($H(\tau)$) was first estimated from the storage modulus (G') with the equation,[33] for $m < 1$,

$$H(\tau) = AG'\, \mathrm{d}(\log G')/\mathrm{d}\left(\log \omega|_{1/\omega=\tau}\right) \quad (4)$$

$$A = \frac{\sin(m\pi/2)}{m\pi/2} \quad (5)$$

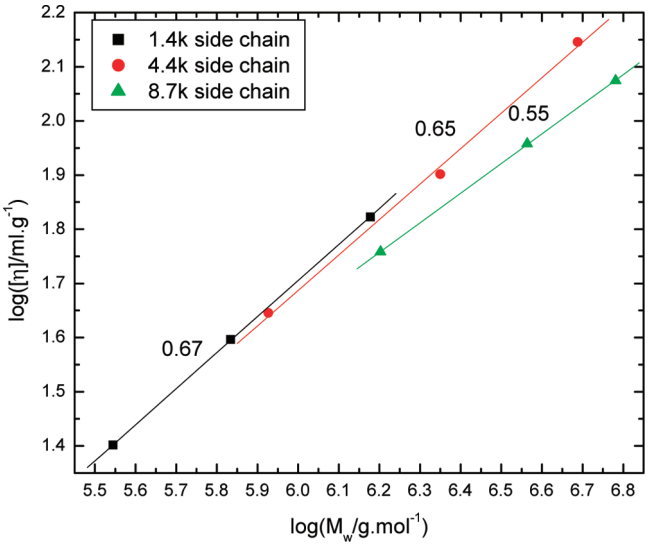

Figure 2. Intrinsic viscosity versus molecular weight for brush polymers with fixed side chain molecular weight but increasing DP (in THF at room temperature ≈ 25 °C).

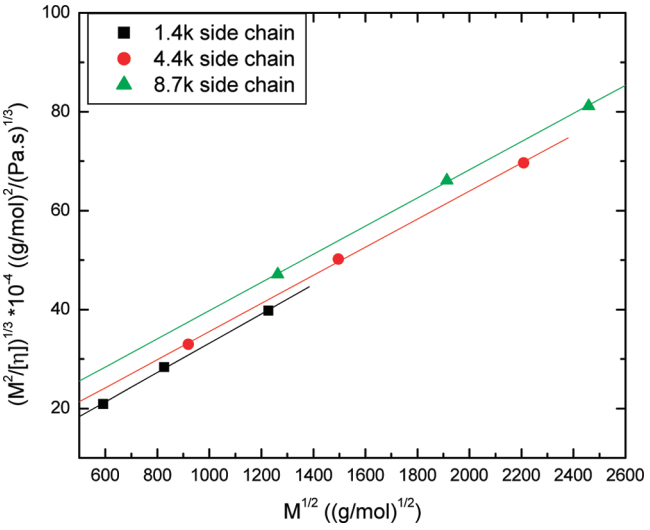

Figure 3. Plot of $(M^2/[\eta])^{1/3}$ vs $M^{1/2}$ for the three groups of brush samples of different side chain length (in THF at room temperature ≈ 25 °C).

for 1 < m<2,

$$H(\tau) = A'G'(2 - \mathrm{d}\left(\log G'\right)/\mathrm{d}(\log \omega)|_{1/\omega=\tau} \quad (6)$$

$$A = \frac{\sin(m\pi/2)}{\pi(1-m/2)} \quad (7)$$

Then L(τ) was calculated from the H(τ) with

$$L(\tau) = \frac{H(\tau)}{[G'(1/\tau) - G''(1/\tau) + 1.37H(\tau)]^2 + \pi^2H^2(\tau)} \quad (8)$$

The retardation spectrum ($L(\tau)$) can be directly estimated from the creep data with equation,[33]

$$L(\tau) = M(-m)\left[J(t) - \frac{t}{\eta_0}\right] \mathrm{d}\left(\log\left[J(t) - \frac{t}{\eta_0}\right]\right)/\mathrm{d}(\log(t)|_{t=\tau}) \quad (9)$$

In the present work, because we did not directly obtain the glassy response in creep experiments, the retardation spectrum ($L(\tau)$) curves were constructed by a combination of the dynamic data using eqs 4−8 and the creep response at 80 °C less t/η_o using eq 9.

RESULTS AND DISCUSSION

Intrinsic Viscosity. The intrinsic viscosity ($[\eta]$) and molecular weight for these brush polymers with different side chain and backbone lengths were measured using GPC coupled with a light scattering detector and a viscometer. As shown in Figure 2, for the three groups of brush samples with fixed side chain molecular weight but increasing DP, the slope of log($[\eta]$) vs log(M_w) decreases from 0.67 to 0.55 as the side chain molecular weight increases. Tsukahara[15] examined the intrinsic viscosity change for a series of poly(MM)s with different length polystyrene (PS) side chains. On the double logarithmic plot of intrinsic viscosity with the total polymer molecular weight, the intrinsic viscosity was found to be unchanged until a critical molecular weight value was reached. Then the intrinsic viscosity was found to increase sharply and scale with the same Mark−Houwink parameter as that for PS in the same conditions. The critical molecular weight for the occurrence of this sudden viscosity change increased with side chain molecular weight.[15] In the present study, the slopes of log($[\eta]$) vs log(M_w) are near and slightly lower than what is expected for PLA in good solvent,[40,41] and the values decrease weakly with increasing side chain molecular weight. Though the data are limited, it appears likely that these polymers are above the region of their critical molecular weight.

The chain conformation of the densely grafted brush polymers can be estimated from their intrinsic viscosity data. The model proposed by Yamakawa[42−44] for the $[\eta]$ and molecular weight of the bottle brush polymers was applied to analyze our data,

$$\left(\frac{M^2}{[\eta]_0}\right)^{1/3} = \Phi_{0,\infty}{}^{-1/3}A_0M_L + \Phi_{0,\infty}{}^{-1/3}B_0\left(\frac{\lambda^{-1}}{M_L}\right)^{-1/2}M^{1/2} \quad (10)$$

M is the chain molecular weight; $[\eta]_0$ is the intrinsic viscosity for unperturbed conditions; $\Phi_{0,\infty}{}^{-1/3}$ is a constant; A_0 and B_0 are functions of the reduced hydrodynamic diameter; M_L is equal to M divided by the contour length (L) and λ^{-1} is the Kuhn length. For chains in good solvent, the expansion of the molecular dimension due to the excluded volume effect should be considered. The viscosity expansion factor is defined as $a_\eta{}^3 = [\eta]/[\eta]_0 = (1 + 3.8z + 1.9z^2)^{0.3}$, where z is the excluded volume parameter. As there is little knowledge about the values of the relevant parameters for the brush polymers used in the present study, we simply plotted the good solvent data of $(M^2/[\eta])^{1/3}$ vs $M^{1/2}$ and from this plot estimated the change of M_L and λ^{-1} from the slope and the intercept (Figure 3).

In Figure 3, the three lines are nearly linear indicating that the influence of the viscosity expansion parameter is not very strong. The intercept ($\Phi_{0,\infty}{}^{-1/3}A_0M_L$) values are 3.5 × 10^{-4}, 7.1 × 10^{-4}, and 11.3 × 10^{-4}. Since in the equation $\Phi_{0,\infty}{}^{-1/3}$ and A_0 are a constant, this indicates that M_L increases with increasing

dx.doi.org/10.1021/ma2009673 |Macromolecules 2011, 44, 6935–6943

side chain molecular weight ($M_{w,side}$ = 1.4, 4.4, and 8.7 kDa). As the molecular weight of the brush polymer is determined by the side chain molecular weight multiplied by the degree of polymerization (DP) of the macromonomers ($M_w \approx M_{w,side} \times DP$), the contour length ($L = M/M_L = M_{w,side}/M_L \times DP$) should be a constant value for brush polymers having the same DP. The slope values ($\Phi_{0,\infty}{}^{-1/3}B_0((\lambda^{-1})/(M_L))^{-1/2}$) determined from Figure 3 for the three groups of samples are nearly constant, which implies that the Kuhn length (λ^{-1}) only increases with the side chain molecular weight and has a fixed value for brush polymers with the same side chain. If we assume the Kuhn length for the 1.4k side chain samples to be k_b, then the Kuhn length for the 4.4k and 8.7k side chain samples are $2.0k_b$ and $3.2k_b$, respectively. The results are similar to what has been well discussed in other work[15,16,21,22,45−47] for brush polymers with densely grafted branches and fixed side chain length. Due to the strong steric interactions between the side chains, the backbone becomes rigid and the Kuhn length of the branched polymer increases.

Dynamic Responses of the Brush Polymers. Figures 4a through 4c present dynamic master curves at 80 °C for the brush polymers having different DPs and side chain molecular weights over the full range from the glassy plateau to the terminal flow region. The master curves are presented as families of fixed backbone DP and varying side chain length. Within a given series of fixed backbone DP the curves are vertically shifted to separate the data for each different side chain length. The figures show clearly that from the glassy state to the terminal flow region, several different relaxation behaviors appear in sequence. In the following sections, we plot the dynamic master curves in different ways and compare the influence of side chain length and backbone DP to the sequential relaxation behaviors of these densely branched brush polymers.

In the terminal zone, most of the densely branched brush samples seem to behave in a Rouse-like manner. There is little evidence of entanglement. For linear polymer materials increasing the backbone length leads to a longer relaxation time and the terminal flow region will move to a lower frequency.[33] On the other hand, in Figure 4, if compare the brush samples with the same backbone DP, the terminal relaxation time not only depends on the DP of the polymer, but also increases with increasing side chain molecular weight. Similar phenomena have been observed for other brush or comb polymers with fixed backbone length and the influence of the side chains on the relaxation of the backbone was invoked to explain this phenomenon.[5]

For the samples with 4.4k and 8.7 kDa side chains, two rubbery plateau regions can be observed in the dynamic master curve. Upon increasing side chain molecular weight, the first plateau from the glassy modulus region at intermediate frequencies becomes more obvious, while the second plateau gradually develops as the DP increases. The two plateau region phenomenon is referred to as a double relaxation mechanism which is typical for brush, comb, or star polymers with long side chains.[1−12]

To clarify the attribution of the two plateaus in the dynamic spectrum for the brush polymers with different side chain molecular weight, the dynamic master curves were plotted following the van Gurp−Palmen method[48] by plotting the phase angle (δ°) vs the logarithm of the complex modulus $|G^*|$. The van Gurp−Palmen plot is sensitive to the molecular weight and molecular architectures of the materials and provides an excellent tool to estimate the value of the plateau modulus.[49] The van

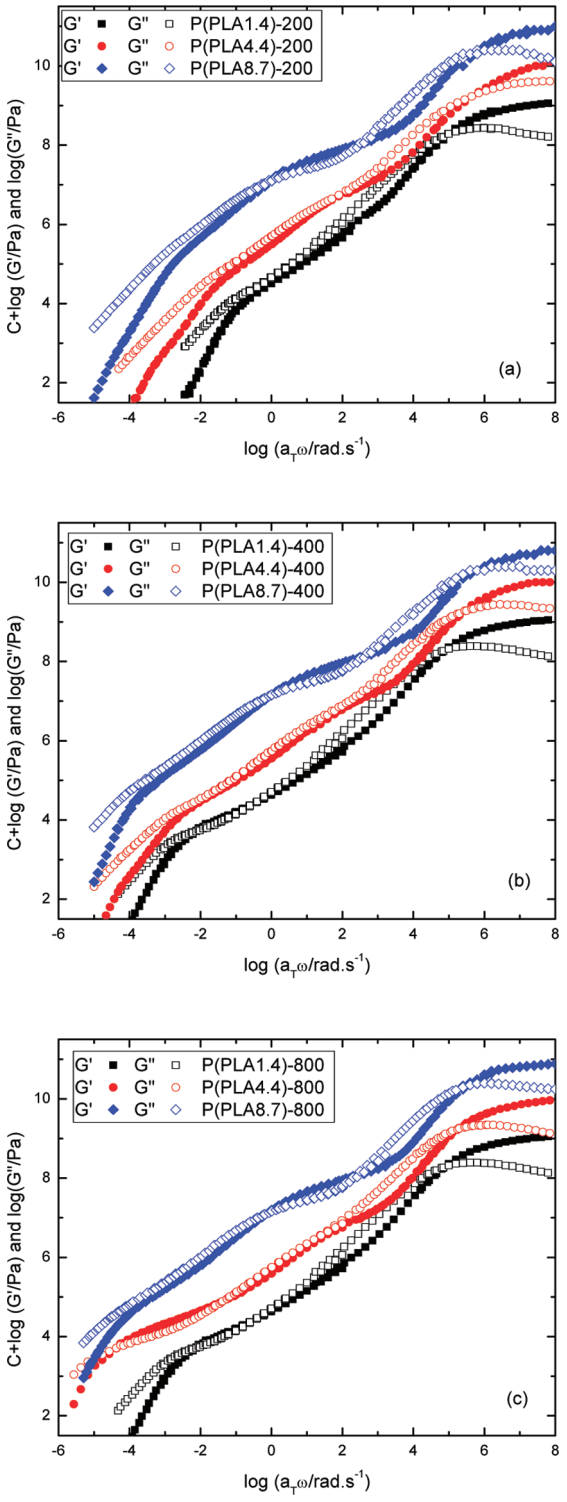

Figure 4. Comparison of the dynamic responses of the investigated brush polymers with fixed DP (200, 400, and 800) (vertical shift of $C = 0$, 1, and 2 used to separate the respective the curves).

Gurp−Palmen plots for the DP dependence and the side chain molecular weight dependence of several brush samples are shown in Figure 5, parts a and b. Similar to the two plateau phenomenon discussed in relation to the dynamic curves, there are two minima in the phase angle (δ) vs log$|G^*|$ plot for most of the brush samples. As shown in Figure 5a, for the first minimum

dx.doi.org/10.1021/ma2009673 |Macromolecules 2011, 44, 6935–6943

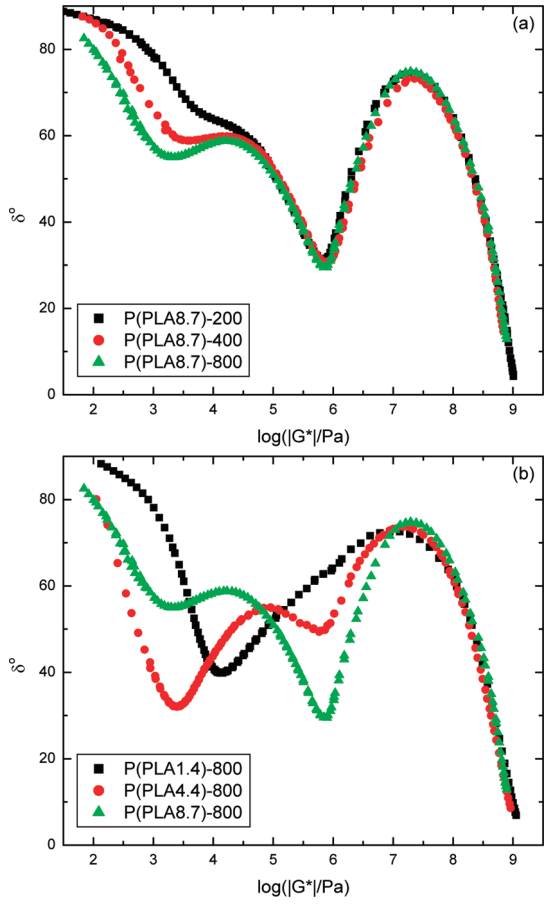

Figure 5. van Gurp−Palmen plot for brush polymers with (a) fixed side chain molecular weight and (b) fixed backbone DP.

in the phase angle (δ) at higher modulus, the $|G^*|$ values and phase angle (δ) values are almost independence of the DP with fixed side chain molecular weight. While in Figure 5b, for fixed backbone DP and increasing side chain molecular weight, the $|G^*|$ values at the first minimum are almost fixed but the δ value decreases. In van Gurp−Palmen plots for linear polymers, as the molecular weight increases, the δ value will decrease and the $|G^*|$ values do not change.[49] Hence, parts a and b of Figure 5 suggest that the first minimum in the van Gurp−Palmen plot, which corresponds to the first plateau in the dynamic master curve, should be related with the relaxation of the side chains. The plateau modulus of the polylactide is reported to be approximately 5×10^5 Pa and the entanglement molecular weight is approximately 8.7 kDa.[50] In parts a and b of Figure 5, the corresponding $|G^*|$values for the first plateau is approximately 6.3×10^5 Pa, which is near to the plateau modulus value for the polylactide.

The second minimum in the van Gurp−Palmen plot gives a modulus value of approximately 2 to 5 kPa. For brush polymers with the same side chain molecular weight as shown in Figure 5a, the δ value at the second minimum decreases with increasing DP. While for the polymers with the same DP but different side chain molecular weight (Figure 5b), the δ value increases with increasing side chain molecular weight. As discussed before, the side chains stiffen the backbone and increase the Kuhn length. We expect that the effect of the side chain on the conformation of the backbone also occurs in the melt[16] and these brush polymers of the same DP

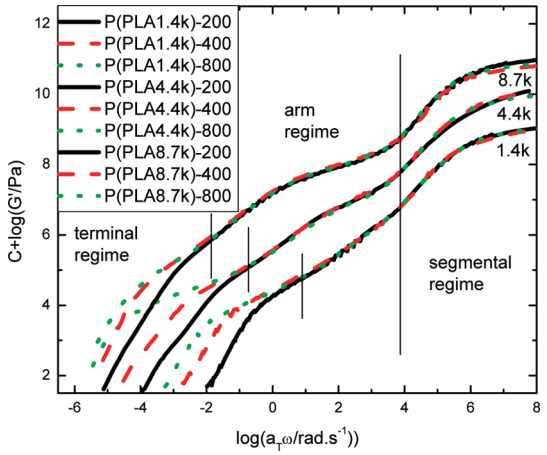

Figure 6. Sequential relaxation of the brush polymers (vertical shift of C = 0, 1, and 2 used to separate the respective the curves).

are unlikely to entangle as the side chain molecular weight increases. The second plateau should, thus, reflect the molecular weight and conformation change of the backbone and it should, consequently, correspond to the relaxation of the whole brush polymer. This lower plateau modulus phenomenon is similar to what has been reported for other poly(macromonomer) brushes[16,19] with longer backbone but shorter side chain than our samples.

Sequential Relaxation. It is expected that branched polymers should relax sequentially. The chain segments should relax first, followed by the side chains, and the whole polymer should be the last to move.[1,3,11] Rheooptical study of a similar densely branched polymer shows relaxation that follows the same sequence as regular branched polymers.[51] To examine the sequential relaxation behaviors of the brush polymers, we plot the storage modulus (G') master curves of brush polymers having the same side chains shifted horizontally to match in the segmental regime. The slight horizontal shifting was applied to compensate for the modest differences in glass transition temperatures among the samples. As shown in Figure 6, the master curves can be divided into three regimes: the segmental regime, the arm regime, and the terminal regime. For the brush polymers with the same side chains, when their glass transition regions are shifted together, the arm regimes overlap with each other very well. The length of the arm regime increases with increasing side chain length. In the terminal region, the curves start to deviate from each other moving to lower frequency as the DP of the backbone increases.

Temperature Dependence of the Dynamic Responses. Figure 7 depicts the temperature shift factors for the three groups of brush polymers with the reference temperature T_{ref} = 80 °C. We fit the shift factors with the WLF equation[34] to obtain the fitting parameters C_1 and C_2 at the reference temperature of 80 °C.

Following the analysis method discussed before, the values for C_1^g, C_2^g, fragility index (m), apparent activation energy (E_g), and glass transition temperature (T_g) of the brush polymers are estimated and listed in Table 2.

For these brush polymers, the fragility values increase with increasing side chain molecular weight, which means the polymer molecules become less flexible as the side chain length increases.[38] As discussed in the section on intrinsic viscosity, the strong

dx.doi.org/10.1021/ma2009673 |*Macromolecules* 2011, 44, 6935–6943

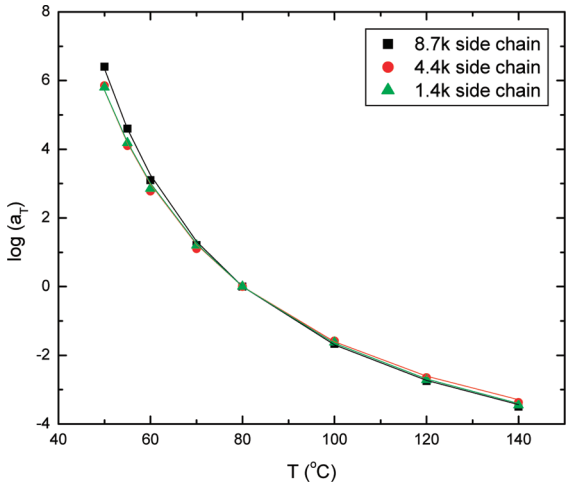

Figure 7. Temperature shift factors for brush polymers with different side chain molecular weight (1.4k, 4.4k, and 8.7k Da) at the reference temperature of 80 °C.

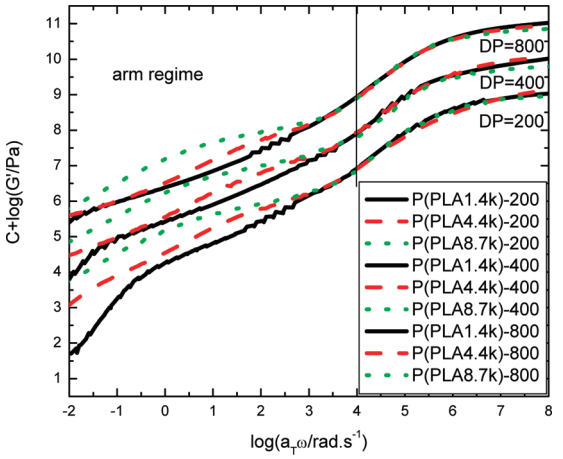

Figure 8. Expanded plot of the arm regime and segmental regime for the brush polymers with fixed DP (vertical shift of $C = 0$, 1, and 2 used to separate the respective DP curves).

Table 2. WLF Fitting Parameters, Fragility, Apparent Activation Energy, and Glass Transition Temperature Determined from the Dynamic Modulus Data for the Brush Polymers

	$C_1^{g\,a}$	$C_2^{g\,a}$(K)	m^b	E_g^c (kJ/mol)	T_g^d (K)
P(PLA1.4)-200	11.22	41.58	88.6	556.4	328.2
P(PLA1.4)-400			88.5	556.1	328.1
P(PLA1.4)-800			88.7	557.8	328.6
P(PLA4.4)-200	11.5	36.06	103.7	645.7	325.2
P(PLA4.4)-400			103.8	646.8	325.5
P(PLA4.4)-800			104.0	649.6	326.2
P(PLA8.7)-200	12.05	34.92	112.5	702.5	326.1
P(PLA8.7)-400			112.4	701.2	325.8
P(PLA8.7)-800			112.7	705.1	326.7

[a] C_1^g and C_1^g are the WLF fit parameters for the brush samples with reference temperature at the glass transition temperature. [b] m is estimated with eq 2. [c] E_g is estimated with eq 3. [d] T_g is the mechanical glass transition temperature at 100 s relaxation time.

interactions among the side chains stiffen the backbone and increase the Kuhn length.[15,16] Here in bulk, we see similar influence of the side chain to the conformation of the polymers. Unlike the work done by others on poly(macromonomers)[16] or comb polymers,[52] the glass transition temperatures (T_g) of our samples are not greatly affected by the side chain length. The glass transition temperature (T_g) and fragility (m) for polylactide are reported to be 323 K and 69.6, respectively.[53] The T_g values estimated for these brush polymers are close and within the glass transition temperature range expected for linear polylactide,[41] which seems to confirm that the side chain properties determine the glass transition behaviors of these poly(macromonomers).[16] However, it is worth remarking that there is a large difference in the fragility index m between the brushes and linear polylactide material, which remains an area for further investigation.

Segmental Regime. The segmental regime covers the glassy and glass transition region of the brush polymers. The glass transition behaviors of these brush polymers have been discussed in the previous section. If one compares the curves in Figure 6 and Figure 8, the side chain length and backbone DP have only minor effects on the glassy moduli (G_g). The glassy modulus value of the brush polymer is around 10^9 Pa which is much higher than that of polynorbornene and is closer to that of linear polylactide.[41]

Arm Regime. Figure 8 shows an expanded plot of the arm regime for the brush polymers with shifting the polymers with the same DP together. By shifting the samples with the same backbone DP together, the influence of arm length on the relaxation behavior of the brush polymer can be readily demonstrated. For each group of samples with the same backbone DP, a clear plateau is seen for samples with the 4.4 kDa and 8.7 kDa side chain. The plateau values are 6.3×10^5 and 6.2×10^5 Pa, which are independent of the arm length and backbone DP. This regime is missing or difficult to detect in the samples with the 1.4 kDa side chain molecular weight.

As shown in Figure 8, the plateau found in the relaxation behaviors of the arm regime are affected by both the faster segmental relaxation and the slower terminal relaxation processes. Rather than using the dynamic data of Figure 8, a better resolution of the arm relaxation can be achieved using the retardation spectra ($L(\tau)$) of the different brush polymers and these were calculated. The retardation spectra of the brush polymers with the same 200 backbone DP but different side chain molecular weight are plotted in Figure 9. Horizontal shifting was applied to overlap the glassy regions and eliminate the effects of the differences between the glass transition temperatures. According to Plazek,[29,30,33] in the retardation spectra of entangled polymers, there are usually two peaks with similar heights. The length between the two peak points corresponds to the length of the rubbery plateau.

In Figure 9, only one peak is found in all of the retardation spectra. With the increase of the side chain molecular weight, a shoulder plateau region can be seen and this increases in length with increasing side chain molecular weight. If one integrates the retardation spectrum over the relaxation time (τ), the shoulder region in the spectrum corresponds to the side chain relaxation as seen in the relevant dynamic curves. The length of the shoulder region can be estimated as the distance between the glass transition region and the transition region from arm relaxation to the terminal relaxation. If the side chains are entangled, then

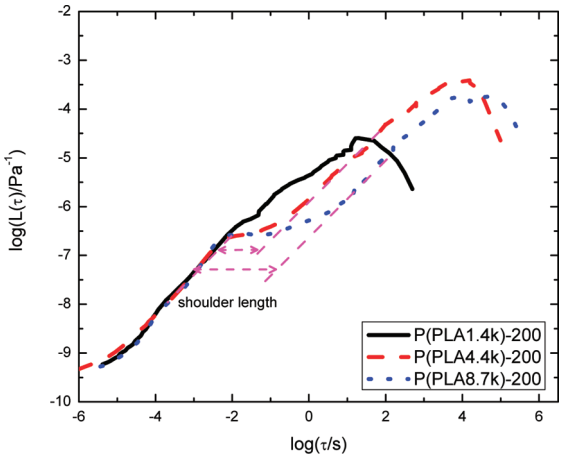

Figure 9. Double logarithmic representation of the retardation spectra ($L(\tau)$) for brush polymers with fixed 200 DP backbone and different side chain molecular weights.

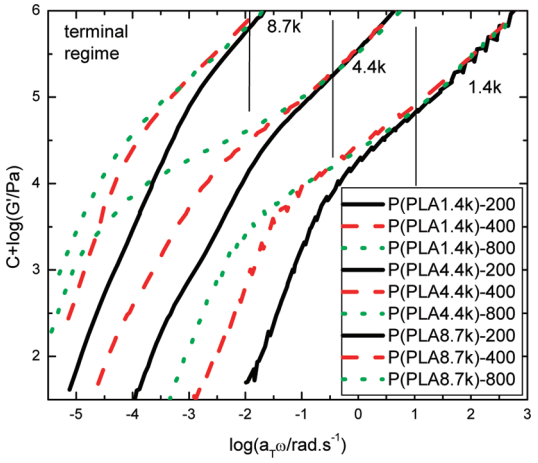

Figure 10. Expanded plot of the terminal regime for the relaxation of the brush polymer with fixed side chains (vertical shift of C = 0, 1, and 2 used to separate the curves).

the length of the shoulder plateau should increase with the 3.4 power of molecular weight.[29] However in Figure 9, the relaxation time only scales approximately as the 2.3 power of the side chain molecular weight, which is consistent with the side chains being unentangled, Rouse-like chains. The unentangled nature and Rouse-like behaviors of side chains are similar to the treatment of the side chains in some current model predictions.[1,12,54,55]

Terminal Regime. Figure 10 presents an expanded plot of the terminal regime and shows the relaxation behavior of the backbone. In the plot, a not very obvious plateau in the storage modulus curve can be found for each sample. This plateau corresponds to the second plateau found in the van Gurp−Palmen plot discussed previously. The modulus values for this plateau can be accurately estimated from the van Gurp−Palmen plot (Table 3). For a polymer network, the shear modulus can be expressed as[56]

$$G = \upsilon kT = \frac{\rho RT}{M_S} \quad (11)$$

υ is the number of network strands per unit volume which is the inverse of the molecular weight of the structure (M_s) included in

Table 3. Estimated Backbone Plateau Modulus (G'_b) and Steady State Recoverable Compliance (J_s) for the Brush Polymers at 80 °C

	$\log(G'_b)$ [a]	$\log(J_s)$ [b]	G'_bJ_s	G'_b ratio [c]
P(PLA1.4)-200	4.64	−4.55	1.2	$3.3G'_{1.4}$
P(PLA1.4)-400	4.38	−4.26	1.3	$1.8G'_{1.4}$
P(PLA1.4)-800	4.12	−3.96	1.4	$1.0G'_{1.4}$
P(PLA4.4)-200	4.11	−4.08	1.1	$5.2G'_{4.4}$
P(PLA4.4)-400	3.72	−3.62	1.3	$2.1G'_{4.4}$
P(PLA4.4)-800	3.39	−3.24	1.4	$1.0G'_{4.4}$
P(PLA8.7)-200	3.96	−3.94	1.0	$4.6G'_{8.7}$
P(PLA8.7)-400	3.62	−3.24	2.4	$2.1G'_{8.7}$
P(PLA8.7)-800	3.30	−3.07	1.7	$1.0G'_{8.7}$

[a] The plateau modulus in the terminal regime estimated using the van Gurp−Palmen plot. [b] Steady state recoverable compliance estimated from the creep data. [c] The ratio of the plateau modulus with different DP.

the relaxation process. In the terminal regime, the whole polymer molecule relaxes. Thus the modulus value should decrease following the same ratio of the increasing DP. As shown in Table 3, the plateau modulus values decrease with increasing DP. If we take the modulus value of the 800DP samples as the reference and mark it as $G'_{1.4}$, $G'_{4.4}$, and $G'_{8.7}$, respectively for different side chains. Then it can be found that, the storage modulus values decrease nearly linearly with increasing DP.

The plateau shown in Figure 10 looks like a rubbery plateau for the brush polymers. However, for an entangled polymer material, the rubbery plateau modulus should be a constant value and independent of the DP.[33] To further examine this, the steady state recoverable compliance (J_s) values for the brush polymers were estimated from the creep experiment data with the equation, $J(t) = J_R(t) + t/\eta$. The $J(t)$ is the shear creep compliance and η is the steady shear viscosity. $J_R(t)$ is the recoverable compliance. According to Plazek,[29,30] for not well entangled polymers, the plateau or shoulder observed in the dynamic modulus data is not the rubbery plateau. It simply reflects the molecular orientation and is not the entropy due to the deformation of a chain entanglement network. The storage modulus value that appears to be a rubbery response in unentangled or lightly entangled linear polymers is indeed the inverse value of the steady state recoverable compliance (J_s). The $G_b'J_s$ is expected to equal 1, and $\log(G_b')$ is equal to the negative $\log(J_s)$. The value of G_b' on this lower plateau is readily estimated from the van Gurp−Palmen plot. If it is the rubbery plateau, theoretically it should be twice the reciprocal of the steady state recoverable compliance ($G_N^0 = 2/J_s$).[33] Thus if the plateau associated with the backbone (G'_b) is not the rubbery plateau, then we expect $\log(J_s) = -\log(G'_b)$. The log values of plateau modulus (G'_b) in the terminal regime estimated from the van Gurp−Palmen plot and steady state recoverable compliance (J_s) obtained from the creep experiments are listed in Table 3.

As shown in Table 3, the value of G'_bJ_s is generally near to Plazek's prediction of 1 for unentangled polymer chains. Thus, following Plazek,[29,30] the backbone plateaus found in the dynamic curves reflect the chain orientation for these stiffened polymers and the plateaus observed are not due to entanglements.

From the above discussion, we did not observe any sign of entanglement in both the arm regime and the terminal regime. Then for these brush polymers of very high molecular weight, are they all Rouse chains? Figure 11 shows the change of the steady

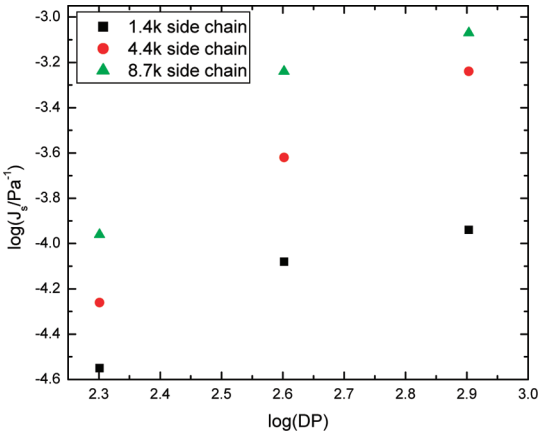

Figure 11. Double logarithmic representation of steady state recoverable compliance (J_s) vs DP for the three groups of brush polymers studied.

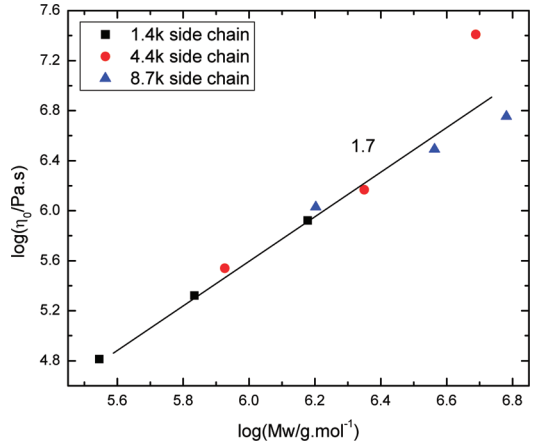

Figure 12. Double logarithmic representation of zero shear viscosity (η_0) at T_g + 30 °C vs weight average molecular weight (M_w) for the three groups of brush polymer samples with different side chain lengths.

state recoverable compliance with DP on a double logarithmic scale. It is assumed that side chains can act as a solvent to dilute the polymer backbone.[3,12] While for linear polymers, solvent dilution effect will increase the J_s values.[57] From Figure 11, we see that for the brush polymers with the same backbone DP, the J_s values increase with side chain length. This shows the increasing dilution effect with side chain length. For the brushes with the same side chain molecular weight but different DP, the steady state recoverable compliance (J_s) increases with DP, and the J_s value is expected to approach a plateau at higher DP. This seems to be the case for the 1.7 kDa and 8.7 kDa side chain brushes, but is less clear for the 4.4 kDa samples. Such a trend is similar to what is expected for linear chains[58] and is consistent with these brushes being in the transition zone from the Rouse like chain to the fully entangled melt.

There are slight differences between the glass transition temperatures (T_g) of these brush polymers. The zero shear viscosities (η_0) at the same experimental temperature therefore do not correctly reflect the viscosity dependence on molecular weight. We use the WLF equation to correct the viscosity value to the same temperature distance from their corresponding glass transition temperatures. To further clarify the entanglement conditions for the brushes in the melt, the zero shear viscosities (η_0) at Tg+30 °C for the three series of samples were plotted against their weight average molecular weights (M_w) and this is shown in Figure 12. The viscosity data can be described with a line with a slope of approximately 1.7, which also indicates that these brush samples are in the transition zone from the unentangled near linear dependence on M_w toward but not reaching entangled behavior.[33]

SUMMARY AND CONCLUSIONS

In this work, three series of densely branched polymers with uniform side chain length and uniform branching point distribution were synthesized via the polymerization of macromonomers using ROMP. Compared with other brush densely grafted polymers, these novel brush polymers have lower polydispersity and a complete grafting of side chains on every backbone repeat unit. The backbone DP of these special brush polymers is in the intermediate range, but the side chains are longer than what had been examined in others' work. Dilute solution characterization shows that the strong intermolecular forces between the side chains cause the Kuhn length of the polymer backbone to increase as the side chains get longer. The densely branched brush polymers with the same backbone DP have the same contour lengths.

A sequential relaxation framework was applied to analyze the relaxation behaviors of these brush polymers. The dynamic modulus master curves of these dense brush polymers were divided into three regions, the segmental regime, arm regime and the terminal regime. Two plateaus were found in the dynamic master curves for the brush polymer with 4.4 kDa and 8.7 kDa side chain. One is in the arm regime and corresponds to the relaxation of the side chain. The other one is in the terminal regime and is related to the movement of the backbone. This double relaxation process phenomenon with one plateau being much lower than the other one is similar to what had been found in other brush polymers with similar structures.

Side chain properties affect the relaxation behavior of the whole brush polymer. For brush polymers with the same side chains but different backbone DP, their arm and segmental regimes are almost identical. The glassy modulus and glass transition temperature are near to the values for the polylactide side chains. The molecular weights of the brush polymers are huge and the side chains are long, however neither the side chains nor the whole polymer show evidence of entanglement. The Rouse-like behaviors of the side chain in the arm regime are confirmed by analyzing the retardation spectra.

A very low modulus plateau can be found in the terminal zone. Both the backbone DP and the arm length can affect the plateau value. Further analysis shows that the plateau is related to the relaxation of the backbone and is not the entanglement or rubbery plateau. It is the inverse value of the steady state recoverable compliance and only reflects the molecular orientation of these Rouse-like chains. The unentangled nature of these brush polymers was further confirmed by the zero shear viscosity in the melt state. The slope of the zero shear viscosity vs weight average molecular weight is much smaller than 3.4, being 1.7, i.e., although having very large molar masses these brush polymer chains remain unentangled.

AUTHOR INFORMATION

Corresponding Author

*E-mail: (G.B.M.) Greg.mckenna@ttu.edu; (J.A.K.) jak@cheme.caltech.edu.

■ ACKNOWLEDGMENT

This research was supported by the U.S. Department of Energy, Office of Basic Energy Sciences, Division of Materials Sciences and Engineering under Award No. DE-FG02-05 ER46218.

■ REFERENCES

(1) Milner, S. T.; McLeish, T. C. B. *Macromolecules* **1997**, *30*, 2159–2166.
(2) van Ruymbeke, E.; Kapnistos, M.; Vlassopoulos, D.; Huang, T. Z.; Knauss, D. M. *Macromolecules* **2007**, *40*, 1713–1719.
(3) Ball, R. C.; McLeish, T. C. B. *Macromolecules* **1989**, *22*, 1911–1913.
(4) Daniels, D. R.; McLeish, T. C. B.; Kant, R.; Crosby, B. J.; Young, R. N.; Pryke, A.; Allgaier, J.; Groves, D. J.; Hawkins, R. J. *Rheol. Acta* **2001**, *40*, 403–415.
(5) Kapnistos, M.; Vlassopoulos, D.; Roovers, J.; Leal, L. G. *Macromolecules* **2005**, *38*, 7852–7862.
(6) McLeish, T. C. B. *Curr. Opin. Solid State Mater. Sci.* **1997**, *2*, 678–682.
(7) McLeish, T. C. B.; Allgaier, J.; Bick, D. K.; Bishko, G.; Biswas, P.; Blackwell, R.; Blottiere, B.; Clarke, N.; Gibbs, B.; Groves, D. J.; Hakiki, A.; Heenan, R. K.; Johnson, J. M.; Kant, R.; Read, D. J.; Young, R. N. *Macromolecules* **1999**, *32*, 6734–6758.
(8) McLeish, T. C. B.; Milner, S. T. *Adv. Polym. Sci.* **1999**, *143*, 195–256.
(9) McLeish, T. C. B.; Larson, R. G. *J. Rheol.* **1998**, *42*, 81–110.
(10) Park, S. J.; Larson, R. G. *J. Rheol.* **2003**, *47*, 199–211.
(11) Lee, J. H.; Orfanou, K.; Driva, P.; Iatrou, H.; Hadjichristidis, N.; Lohse, D. J. *Macromolecules* **2008**, *41*, 9165–9178.
(12) Wang, Z. W.; Chen, X.; Larson, R. G. *J. Rheol.* **2010**, *54*, 223–260.
(13) Sheiko, S. S.; Sumerlin, B. S.; Matyjaszewski, K. *Prog. Polym. Sci.* **2008**, *33*, 759–785.
(14) Namba, S.; Tsukahara, Y.; Kaeriyama, K.; Okamoto, K.; Takahashi, M. *Polymer* **2000**, *41*, 5165–5171.
(15) Tsukahara, Y.; Kohjiya, S.; Tsutsumi, K.; Okamoto, Y. *Macromolecules* **1994**, *27*, 1662–1664.
(16) Tsukahara, Y.; Namba, S.-i.; Iwasa, J.; Nakano, Y.; Kaeriyama, K.; Takahashi, M. *Macromolecules* **2001**, *34*, 2624–2629.
(17) Berry, G. C.; Kahle, S.; Ohno, S.; Matyjaszewski, K.; Pakula, T. *Polymer* **2008**, *49*, 3533–3540.
(18) Neugebauer, D.; Zhang, Y.; Pakula, T.; Sheiko, S. S.; Matyjaszewski, K. *Macromolecules* **2003**, *36*, 6746–6755.
(19) Pakula, T.; Zhang, Y.; Matyjaszewski, K.; Lee, H. I.; Boerner, H.; Qin, S. H.; Berry, G. C. *Polymer* **2006**, *47*, 7198–7206.
(20) Ying, Z.; Costantini, N.; Mierzwa, M.; Pakula, T.; Neugebauer, D.; Matyjaszewski, K. *Polymer* **2004**, *45*, 6333–6339.
(21) Nakamura, Y.; Wan, Y.; Mays, J. W.; Iatrou, H.; Hadjichristidis, N. *Macromolecules* **2000**, *33*, 8323–8328.
(22) Terao, K.; Farmer, B. S.; Nakamura, Y.; Iatrou, H.; Hong, K.; Mays, J. W. *Macromolecules* **2005**, *38*, 1447–1450.
(23) Wintermantel, M.; Gerle, M.; Fischer, K.; Schmidt, M.; Wataoka, I.; Urakawa, H.; Kajiwara, K.; Tsukahara, Y. *Macromolecules* **1996**, *29*, 978–983.
(24) Zhang, M.; Müller, A. H. E. *J. Polym. Sci., Part A* **2005**, *43*, 3461–3481.
(25) Sheiko, S. S.; Möller, M. *Chem. Rev.* **2001**, *101*, 4099–4124.
(26) Xia, Y.; Olsen, B. D.; Kornfield, J. A.; Grubbs, R. H. *J. Am. Chem. Soc.* **2009**, *131*, 18525–18532.
(27) Xia, Y.; Kornfield, J. A.; Grubbs, R. H. *Macromolecules* **2009**, *42*, 3761–3766.
(28) Ito, K.; Kawaguchi, S. *Adv. Polym. Sci.* **1999**, *142*, 129–178.
(29) Plazek, D. J. *J. Rheol.* **1992**, *36*, 1671–1690.
(30) Plazek, D. J.; Echeverria, I. *J. Rheol.* **2000**, *44*, 831–841.
(31) Marrero, J.; Gani, R. *Fluid Phase Equilib.* **2001**, *183*, 183–208.
(32) Hutcheson, S. A.; McKenna, G. B. *J. Chem. Phys.* **2008**, *129*, 074502–14.
(33) Ferry, J. D. *Viscoelastic properties of polymers*. Wiley: New York, 1980.
(34) Williams, M. L.; Landel, R. F.; Ferry, J. D. *J. Am. Chem. Soc.* **1955**, *77*, 3701–3707.
(35) Angell, C. A. *J. Non-Cryst. Solids* **1985**, *73*, 1–17.
(36) Plazek, D. J.; Ngai, K. L. *Macromolecules* **1991**, *24*, 1222–1224.
(37) Wang, L.-M.; Angell, C. A.; Richert, R. *J. Chem. Phys.* **2006**, *125*, 074505–8.
(38) Qin, Q.; McKenna, G. B. *J. Non-Cryst. Solids* **2006**, *352*, 2977–2985.
(39) Simon, S. L.; Plazek, D. J.; Sobieski, J. W.; McGregor, E. T. *J. Polym. Sci., Part B* **1997**, *35*, 929–936.
(40) Garlotta, D. *J. Polym. Environ.* **2001**, *9*, 63–84.
(41) Mark, J. E. *Polymer Data Handbook*; Oxford University Press: New York: 1999.
(42) Yamakawa, H. *Modern theory of polymer solutions*; Harper & Row: New York, 1971.
(43) Yamakawa, H.; Yoshizaki, T. *J. Chem. Phys.* **1981**, *75*, 1016–1030.
(44) Yamakawa, H.; Yoshizaki, T. *Macromolecules* **1980**, *13*, 633–643.
(45) Terao, K.; Nakamura, Y.; Norisuye, T. *Macromolecules* **1999**, *32*, 711–716.
(46) Terao, K.; Hokajo, T.; Nakamura, Y.; Norisuye, T. *Macromolecules* **1999**, *32*, 3690–3694.
(47) Nemoto, N.; Nagai, M.; Koike, A.; Okada, S. *Macromolecules* **1995**, *28*, 3854–3859.
(48) van Gurp, M.; Palmen, J. *Rheol. Bull.* **1998**, *67*, 5–8.
(49) Trinkle, S.; Friedrich, C. *Rheol. Acta* **2001**, *40*, 322–328.
(50) Dorgan, J. R.; Williams, J. S.; Lewis, D. N. *J. Rheol.* **1999**, *43*, 1141–1155.
(51) Inoue, T.; Matsuno, K.; Watanabe, H.; Nakamura, Y. *Macromolecules* **2006**, *39*, 7601–7606.
(52) Reimschuessel, H. K. *J. Polym. Sci.: Polym. Chem. Ed.* **1979**, *17*, 2447–2457.
(53) Zuza, E.; Ugartemendia, J. M.; Lopez, A.; Meaurio, E.; Lejardi, A.; Sarasua, J. R. *Polymer* **2008**, *49*, 4427–4432.
(54) Larson, R. G. *Macromolecules* **2001**, *34*, 4556–4571.
(55) van Ruymbeke, E.; Bailly, C.; Keunings, R.; Vlassopoulos, D. *Macromolecules* **2006**, *39*, 6248–6259.
(56) Rubinstein, M.; Colby, R. H. *Polymer Physics*; Oxford University Press: New York, 2003.
(57) Ngai, K. L.; Plazek, D. J.; O'Rourke, V. M. *Macromolecules* **1997**, *30*, 5450–5456.
(58) McKenna, G. B.; Hostetter, B. J.; Hadjichristidis, N.; Fetters, L. J.; Plazek, D. J. *Macromolecules* **1989**, *22*, 1834–1852.